

First-principles prediction of post-pyrite phase transitions in germanium dioxide

Haruhiko Dekura (出倉春彦),¹ Taku Tsuchiya (土屋卓久),² and Jun Tsuchiya (土屋旬)¹

¹Senior Research Fellow Center, Ehime University, 2-5 Bunkyo-cho, Matsuyama, Ehime 790-8577, Japan

²Geodynamics Research Center, Ehime University, 2-5 Bunkyo-cho, Matsuyama, Ehime 790-8577, Japan

(Received 14 September 2010; revised manuscript received 6 January 2011; published 12 April 2011)

Two high-pressure phase transitions in GeO_2 have been discovered through first-principles computer simulations: the first is a transition from the pyrite-type (FeS_2) to cotunnite-type ($\alpha\text{-PbCl}_2$) structure predicted to occur at a pressure of ~ 300 GPa, and the second is a transition from the cotunnite-type to the hexagonal Fe_2P -type structure at ~ 600 GPa. The former is accompanied by a remarkable volume reduction of 5.4%, while the latter has a distinctive but quite small volume change of 0.3%. The post-pyrite transition to the cotunnite-type structure is expected from known high-pressure behavior of other dioxides, while the post-cotunnite transition to an Fe_2P -type structure is quite unexpected, with no report in any dioxides so far except for a recent study on SiO_2 . The Fe_2P -type phase has higher effective coordination numbers of Ge atoms, which contributes to stabilizing this structure relative to cotunnite. The results obtained extend our knowledge of the ultrahigh-pressure crystallography of dioxide materials.

DOI: 10.1103/PhysRevB.83.134114

PACS number(s): 64.70.K-, 81.40.Vw, 81.30.Bx

I. INTRODUCTION

Great interest in the high-pressure phase transitions in germanium oxide, GeO_2 , comes from the possible fundamental solid-state physical, geophysical and planetary physical repercussions.^{1–5} Extensive theoretical and experimental studies elucidated that the rutile-type ambient pressure phase subsequently transforms to CaCl_2 ,^{1,2} $\alpha\text{-PbO}_2$,^{3,5} and pyrite (FeS_2)-type phases^{3,4} from 30 to 90 GPa. These phase relations are quite analogous to those of silicon dioxide, SiO_2 ,^{6–8} but the transition pressures are considerably lower in GeO_2 . The cation has a coordination number (CoN) of 6 in all of these structures, and, to the best of our knowledge, no further high-pressure phase transition has been identified as of yet for GeO_2 . In contrast, the cotunnite ($\alpha\text{-PbCl}_2$)-type structure is reported to be the post-pyrite phase in several metal dioxides, including CeO_2 ,⁹ ZrO_2 , HfO_2 ,¹⁰ TiO_2 ,¹¹ TeO_2 ,¹² and SnO_2 ,¹³ which has a cation site with a CoN of 9, the highest reported in oxides, and was also proposed for a high-pressure phase of SiO_2 .^{7,14} However, a more recent study elucidated a different ultrahigh-pressure structure with an unexpected hexagonal Fe_2P -type structure in SiO_2 bypassing the cotunnite stability at static conditions.¹⁵ Since this structure has never been tested in other compounds including GeO_2 , it is of great importance which of the cotunnite-type or Fe_2P -type structure is applicable to a post-pyrite phase in GeO_2 . In this study, we investigate the post-pyrite ultrahigh-pressure phase of GeO_2 by means of *ab initio* density-functional computations.

II. COMPUTATIONAL METHODS

Our computations are based on the density-functional theory^{16,17} within the local density approximation (LDA)^{18,19} and the generalized gradient approximation (GGA).²⁰ To avoid core overlapping under strong compressions, we carefully constructed ultrasoft pseudopotentials²¹ with small core radii, similarly to the previous study,¹⁵ including a semicore of the Ge 3*d* state.²² This treatment required a relatively large kinetic-energy cutoff of 70 Ry for a convergence in electronic structures even using the ultrasoft scheme. The other technical

details are basically the same as those in our previous studies.^{23,24} Calculations were carried out using the QUANTUM ESPRESSO distribution.²⁵ To obtain full convergence in total energies, pressures, and atomic forces, we applied the Monkhorst-Pack method²⁶ to sample on $4 \times 4 \times 6$, $4 \times 6 \times 2$, and $4 \times 4 \times 4$ *k*-point grids in irreducible wedges of Brillouin zones (IBZ) of the Fe_2P , cotunnite, and pyrite-type structures, respectively. We also carried out structural optimizations for other low-pressure structures stabilizing below 100 GPa with *k*-point samplings on $2 \times 2 \times 4$, $4 \times 4 \times 4$, $4 \times 4 \times 4$, and $2 \times 4 \times 4$ grids for IBZs of rutile, $\alpha\text{-PbO}_2$, baddeleyite, and orthorhombic-I-type structures, respectively. We confirmed that these calculation conditions produced a sufficient total energy convergence less than 1 mRy/ GeO_2 for each structure. The structural optimization was performed until the residual force and stress became less than 10^{-5} Ry/a.u. and 0.01 GPa. The phonon frequencies of pyrite-type, cotunnite-type, and Fe_2P -type phases were determined by diagonalizing dynamical matrices that were computed based on the density-functional perturbation theory (DFPT).²⁷ The *q* points on $4 \times 4 \times 4$ grids were sampled for pyrite-type, cotunnite-type, and Fe_2P -type phases, and then force-constant matrices on finer *q*-point grids were calculated by using the Fourier interpolation.

III. RESULTS AND DISCUSSION

Figure 1 depicts the crystal structures of pyrite, cotunnite, and Fe_2P -type GeO_2 , which have a cubic, orthorhombic, and hexagonal lattice with space groups $Pa\bar{3}$, $Pnma$, and $P6_2m$, respectively.^{15,28} These structures are specified by two parameters of *a* and *x*₀₁ for pyrite, nine parameters of *a*, *b*/*a*, *c*/*a*, and *x* and *z* coordinates of Ge, O1, and O2 for cotunnite, and four parameters of *a*, *c*/*a*, *x*₀₁, and *x*₀₂ for Fe_2P (Table I). In the Fe_2P structure, two nonequivalent sites of P are occupied by Ge atoms. Each Ge atom bonds to nine O atoms sitting in the sites of Fe, which form a tricapped trigonal prism. These polyhedra connect each other by sharing edges along the *a* direction and by sharing faces along the *c* direction, making two different chains parallel to the *c* axis and consequently a significant packing lattice.

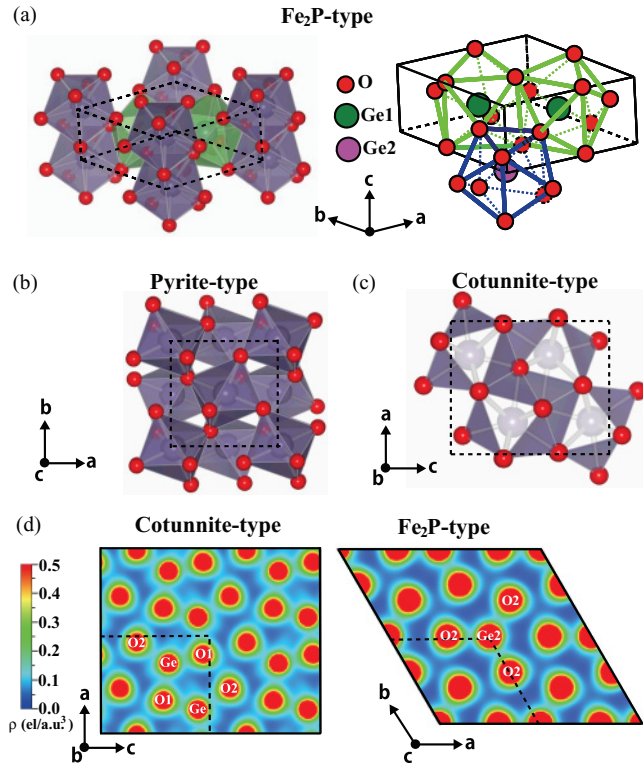


FIG. 1. (Color online) Crystal structures of high-pressure polymorphs of GeO_2 . The hexagonal Fe_2P -type structure with two different kinds of GeO_4 polyhedra (a), pyrite-type (b), and cotunnite-type (c). Red circles and purple (or green) polyhedra indicate oxygen atoms and GeO_4 , respectively. Valence charge densities on the cotunnite (040) and Fe_2P (001) sections calculated within the LDA at 600 GPa are plotted in (d).

Calculated static enthalpy differences, ΔH , of several structure models relative to the pyrite-type phase are plotted in Fig. 2(a) as a function of pressure. Below 100 GPa, a phase sequence of rutile (CaCl_2) \rightarrow α - PbO_2 \rightarrow pyrite is obtained, which

is in complete agreement with reported results^{3–5} including transition pressures of 36 and 63 GPa for the first and second transitions, respectively. In the further multimegabar pressure region, the static enthalpies indicate first a phase transition from the pyrite-type to cotunnite-type structure found to occur at 280 GPa [Fig. 2(a)], and second a further transition from the cotunnite-type to Fe_2P -type structure at 589 GPa [inset in Fig. 2(a)]. Calculated enthalpies of cotunnite and Fe_2P are relatively comparable, but that of Fe_2P clearly decreases faster than that of cotunnite with increasing pressure, and those finally cross at 589 GPa. This high-pressure phase relationship in GeO_2 is quite analogous to that reported in silica, but silica was reported to have no stability field of the cotunnite-type phase at static conditions.¹⁵ We also examined these phase relationships using GGA,²⁰ by which the same phase sequence was identified. The transition pressure from cotunnite to Fe_2P was found to be 611 GPa, ~ 20 GPa higher than by the LDA, while the transition pressure from pyrite to cotunnite was 281 GPa, quite comparable to the LDA calculation. It is considered that differences between the LDA and the GGA decrease under strong compression, when the charge density delocalizes and becomes more homogeneous. However, the difference in the transition pressures to Fe_2P -type GeO_2 obtained within the LDA and the GGA suggests that the gradient corrections for the inhomogeneous charge density related to the localizing Ge-O bonds still remain substantial even at these pressures.

To the best of our knowledge, these two phase transitions in GeO_2 have not been reported. In particular, this is the second example for evidence of the stabilization of the Fe_2P -type structure among any dioxide compounds next to SiO_2 . The cotunnite and Fe_2P -type structures both consist of GeO_4 tricapped trigonal prisms with their dense connectivity. A polyhedral occupancy ($\Sigma V_{\text{poly}}/V_{\text{cell}}$) in the Fe_2P structure is found to be much larger than in the pyrite structure and a bit larger than in the cotunnite structure, as shown in Table I. In contrast, we found unexpectedly long interatomic

TABLE I. Crystallographic properties calculated within the LDA for the pyrite-type at 300 GPa, cotunnite-type at 600 GPa, and Fe_2P -type at 600 GPa. The GGA values are also given in parentheses.

Structure (Space group)	Cell parameter (Å)	V_{cell} (Å ³)	V_{poly} (Å ³)	$\Sigma V_{\text{poly}}/V_{\text{cell}}$	Atomic position (x,y,z)
Pyrite ($Pa\bar{3}$, No. 205) $P = 300$ GPa	a 4.060 (4.377)	66.92 (68.47)	5.909 (6.099)	0.353 (0.356)	Ge 4a 0, 0, 0 O 8c 0.353, 0.353, 0.353 (0.352, 0.352, 0.352)
Cotunnite ($Pnma$, No. 62) $P = 600$ GPa	a 4.221 (4.247) b 2.540 (2.552) c 4.995 (5.029)	53.55 (54.50)	10.52 (10.71)	0.786 (0.786)	Ge 4c 0.252, 1/4, 0.883 (0.252, 1/4, 0.883) O1 4c 0.350, 1/4, 0.571 (0.351, 1/4, 0.571) O2 4c 0.478, 1/4, 0.174 (0.478, 1/4, 0.174)
Fe_2P ($P\bar{6}2m$, No. 189) $P = 600$ GPa	a 4.351 (4.377) c 2.442 (2.456)	40.03 (40.76)	10.93 (Ge1O_9) (11.12) 9.801 (Ge2O_9) (9.98)	0.791 (0.791)	Ge1 2d 1/3, 2/3, 1/2 Ge2 1a 0, 0, 0 O1 3g 0.257, 0, 1/2 (0.257, 0, 1/2) O2 3f 0.589, 0, 0 (0.587, 0, 0)

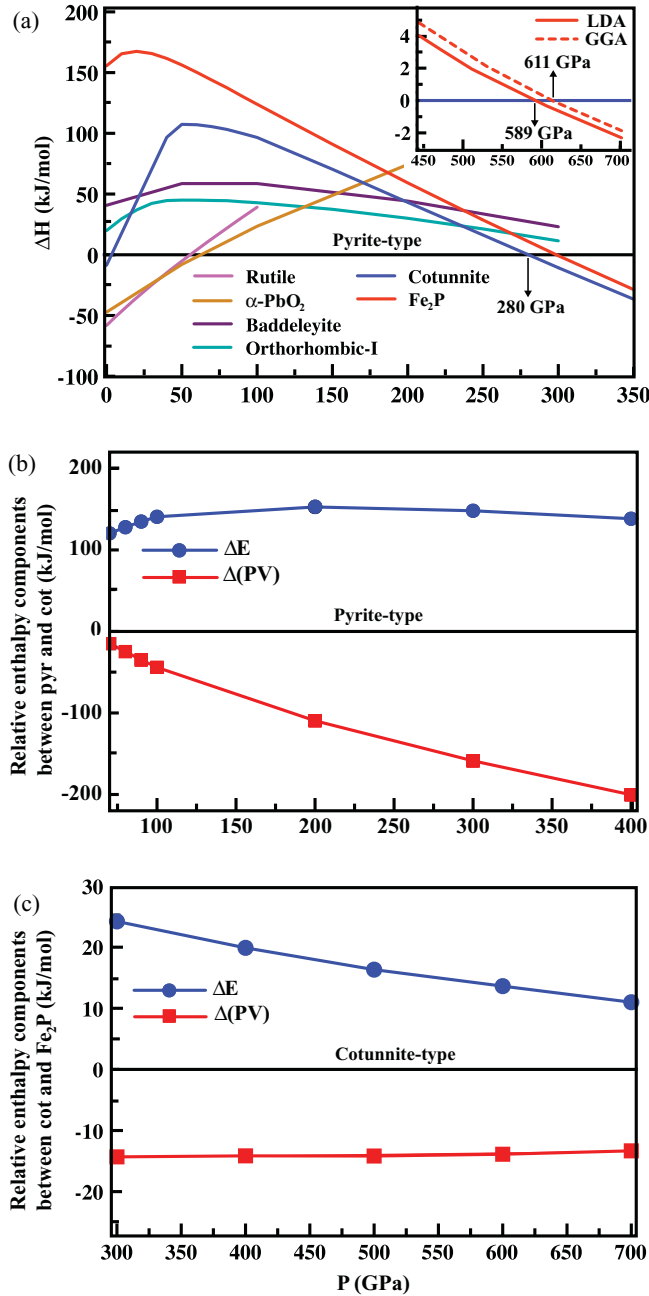


FIG. 2. (Color online) Calculated static enthalpy differences as a function of pressure relative to the pyrite-type structure (a) and relative to the cotunnite-type structure (inset). Results obtained within the GGA (Ref. 20) are also shown. The GGA shifts the post-cotunnite transition pressure higher, but only marginally affects the post-pyrite transition pressure. Pressure dependencies of two components in enthalpy differences, ΔE_{tot} and $\Delta(PV)$, between pyrite and cotunnite and between cotunnite and Fe_2P are presented in (b) and (c), respectively.

Ge-O distances in the cotunnite and Fe_2P structures with mean values of 1.735 and 1.722 Å at 600 GPa, respectively. These are notably longer than 1.661 Å in pyrite even at 300 GPa. These results clearly mean that the volume contraction in cotunnite and Fe_2P is predominantly achieved by the dense polyhedral connectivity and not by compression of the distance between nearest neighbors. Note that these crystallographic

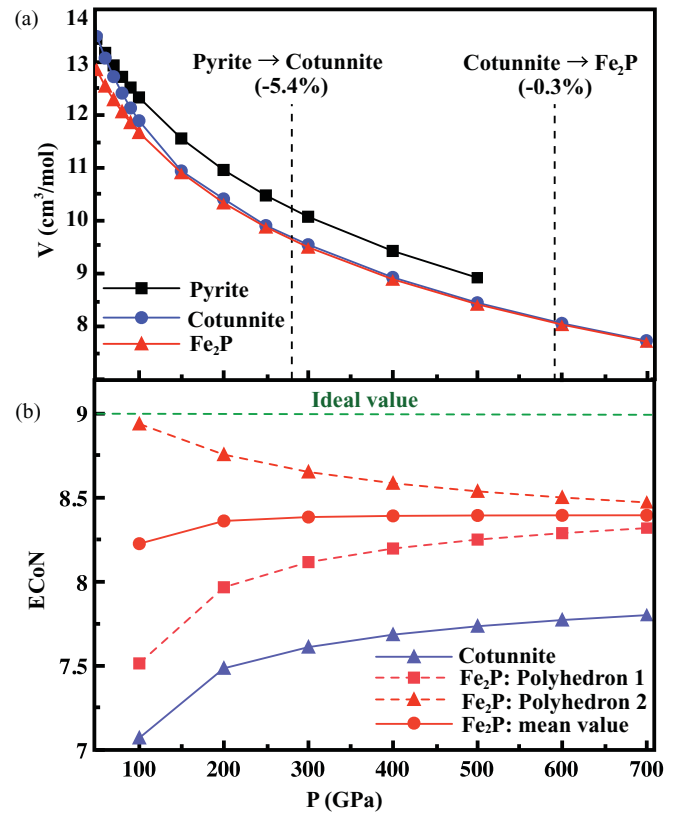


FIG. 3. (Color online) Compression behaviors calculated within the LDA. The volume-pressure relationships of pyrite (black line), cotunnite (blue), and Fe_2P -type (red) structures are shown in (a). The two transition pressures are specified by vertical dashed lines with the volume contrasts across the phase changes in parentheses. Variations in the effective coordination numbers (ECoN) (Ref. 30) of FeO_9 tricapped trigonal prisms in the cotunnite and Fe_2P -type structures are shown in (b).

characteristics of the Fe_2P -type phase are almost identical to those reported in SiO_2 .¹⁵

Calculated volume compression curves of the pyrite, cotunnite, and Fe_2P -type GeO_2 are plotted in Fig. 3(a). Equation of state (EOS) parameters evaluated for the three high-pressure GeO_2 phases are given in Table II. For the cotunnite-type and Fe_2P -type, large volume expansions are found under decompression. This is due to substantial expansions of the tricapped trigonal prisms, leading to the zero-pressure bulk moduli of both structures substantially smaller than that of the pyrite-type

TABLE II. Equation-of-state parameters (zero-pressure volumes, bulk moduli, and their pressure derivatives) determined by fitting to the third-order Birch-Murnaghan EOS. The GGA values are also given in parentheses.

Structure	V_0 (Å ³ /cell)	B_0 (GPa)	B'_0
Pyrite	101.63	294.9	4.22
	(110.81)	(203.5)	(4.42)
Cotunnite	116.78	103.35	5.02
	(131.17)	(66.2)	(5.25)
Fe_2P	77.395	185.0	4.76
	(87.351)	(105.8)	(5.20)

(Table II). However, Fig. 3(a) indicates that the compressibility of the cotunnite-type and Fe_2P -type phases becomes almost comparable to that of the pyrite-type over 150 GPa, and that the volumes of cotunnite-type and Fe_2P -type phases are considerably smaller than that of the pyrite-type. The volume contrast between the pyrite-type and cotunnite-type is considerable, reaching -5.4% . In contrast, the volumes of cotunnite and Fe_2P -type phases are again fairly comparable, as is expected from the same coordination environment around Ge ions in those structures. We found a marginal volume change (-0.3%) across the post-cotunnite transition. These imply different transition mechanisms in the two phase changes. As is usually seen,²⁹ the GGA provided larger volumes and thus smaller bulk moduli for all the phases than does the LDA. However, we found that the GGA gives structural properties such as atomic coordinates and polyhedral occupancies quite similar to those of the LDA (Table I). The volume contrasts between the pyrite-type and cotunnite-type at 300 GPa and between the cotunnite-type and Fe_2P -type at 600 GPa are also quite similar: -5.2% and -0.3% , respectively.

Static enthalpy has two different components represented as $H(P) = E_{\text{tot}}(P) + PV$, where E_{tot} is the electronic total energy. To clarify the thermodynamic details of the phase changes, we investigated contributions of these two terms separately, as demonstrated in Figs. 2(b) and 2(c). The differences in these terms of the pyrite-type and cotunnite-type show that $\Delta(PV)$ decreases with pressure while the total energy difference, ΔE_{tot} , is almost constant [Fig. 2(b)], indicating that the enthalpy crossover is achieved primarily by the contribution of the volume contraction. In contrast, the differences between the cotunnite and Fe_2P -type phases show that ΔE_{tot} decreases with pressure while $\Delta(PV)$ is almost constant [Fig. 2(c)], indicating that the enthalpy crossover in this case is achieved primarily by the difference in electronic contributions, in other words by a total energy gain.

To understand this behavior of the total energy difference between the cotunnite and Fe_2P -type structures, we analyzed first the local coordination environment in more detail. This was performed first by considering the so-called effective coordination number (ECoN),³⁰ defined as $\sum_j 1 - (l_j/l)^6$, where $l = \sum_j l_j \exp[1 - (l_j/l_{\text{min}})^6]$ is the weighted mean bond length with the shortest length l_{min} . Pressure dependences of calculated ECoN in the cotunnite and Fe_2P -type structures are demonstrated in Fig. 3(b). Since the Fe_2P -type structure has two different Ge sites, there are two kinds of ECoN corresponding to each site. ECoNs for both sites in Fe_2P and also their average are found to be larger and closer to the apparent CoN of 9 compared to that of cotunnite. This means that the GeO_9 tricapped trigonal prisms in the Fe_2P structure are more regular and ideal than those in cotunnite, which makes the mean Ge-O distance in Fe_2P (1.722 Å at 600 GPa) a little shorter than in cotunnite (1.735 Å), leading to a bulk volume smaller in Fe_2P , as mentioned above.

We also attempted to understand the difference in the stability of cotunnite and Fe_2P due to aspects of their electronic properties. To do this, the Bader charge-density analysis³¹ was performed. Figures 4(a) and 4(b) show the calculated effective charges of Ge and O atoms in pyrite, cotunnite, and Fe_2P structures as a function of pressure. The charge of Ge in those structures decreased as pressure increased. At

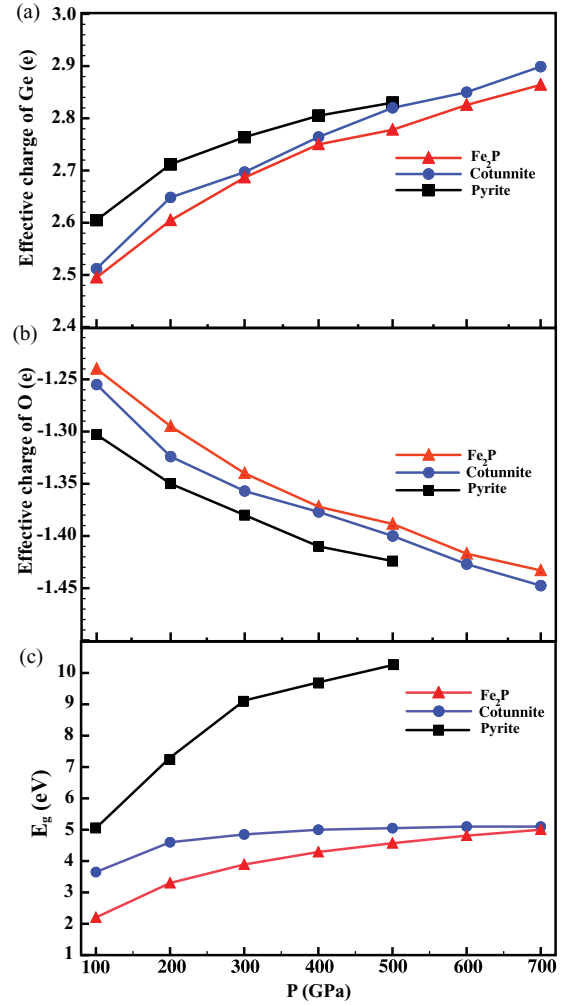


FIG. 4. (Color online) Electronic properties obtained within the LDA. Pressure dependences of the Bader effective charges³¹ of Ge (a) and O atoms (b) in pyrite, cotunnite, and Fe_2P structures and energy gaps (E_g) of those structures (c). Red, blue, and black lines represent the values for the Fe_2P -type, cotunnite-type, and pyrite-type phases.

300 GPa, we obtained the effective charges of Ge and O atoms of $+2.76e$ and $-1.38e$ in pyrite-type and $+2.70e$ and $-1.35e$ in cotunnite-type, respectively. At 600 GPa, the effective charges of Ge and O atoms are $+2.86e$ and $-1.43e$ in cotunnite-type and $+2.82e$ and $-1.41e$ in Fe_2P -type, respectively. Therefore, the Ge-O bond is suggested to be more ionic in pyrite than in cotunnite, and slightly more ionic in cotunnite than in Fe_2P , indicating that the ionicity decreases with the phase transitions. The calculated band gaps (E_g) are plotted in Fig. 4(c). E_g decreases substantially from 9.1 to 4.9 eV across the pyrite-to-cotunnite transition at 300 GPa, corresponding to the relatively large change in ionicity [Figs. 4(b) and 4(c)]. In contrast, we obtained a small change in E_g across the transition from cotunnite-type (5.1 eV) to Fe_2P -type (4.8 eV), which is also consistent with the small decrease in the effective charges. DFT is widely known to systematically underestimate the band gap of insulators,³² but their relative differences in the different phases are likely evaluated appropriately. The small differences in the ionicity and E_g between the cotunnite and Fe_2P -type phases may be related to the ideality of the

coordination polyhedra. Valence charge densities of cotunnite and Fe_2P illustrated in Fig. 1(d) indicate that the charge density around oxygen ions deforms to reside on the Ge-O bonds due to some covalency. They clearly show that the coordination polyhedra are less distorted in Fe_2P than in cotunnite. Covalent

bonds generally stabilize more in the more regular polyhedra with smaller distortions of bond angles and bond distances, so that the total energy gets lower in the Fe_2P -type structure with more regular GeO_9 tricapped trigonal prisms. The GGA also produced similar properties of the Bader charges and

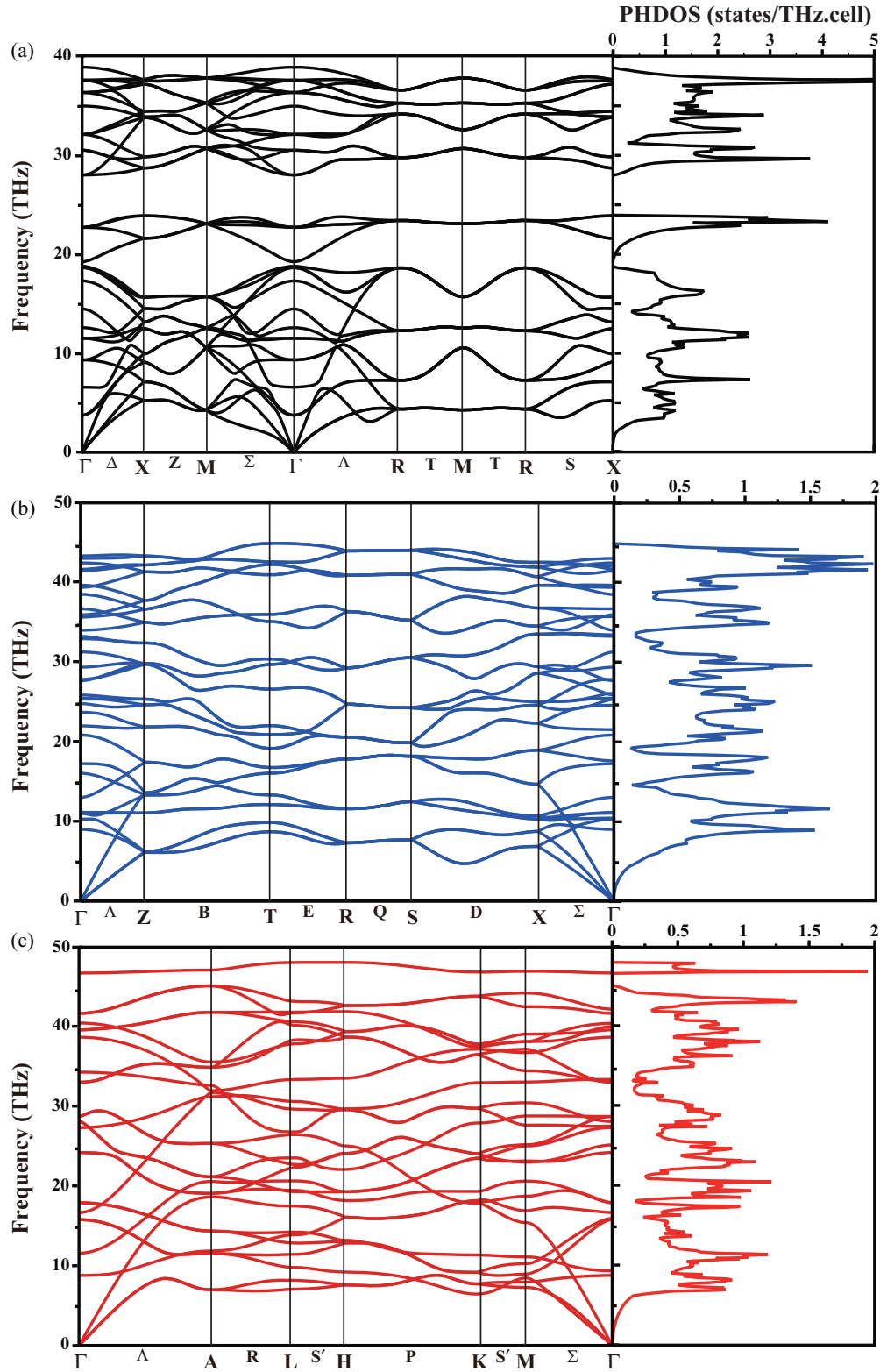


FIG. 5. (Color online) Phonon-dispersion relations calculated within the LDA for the pyrite-type at 300 GPa (a), cotunnite-type at 600 GPa (b), and Fe_2P -type structures at 600 GPa (c).

E_g , but it gives comparable effective charges of Ge and O atoms: $+2.84e$ and $-1.42e$ in pyrite-type and $+2.76e$ and $-1.38e$ in cotunnite-type at 300 GPa, and $+2.90e$ and $-1.45e$ in cotunnite-type and $+2.86e$ and $-1.43e$ in Fe_2P -type at 600 GPa respectively. The E_g obtained within the GGA are also comparable to the LDA values and decreased from 8.4 eV (pyrite-type) to 5.1 eV (cotunnite-type) at 300 GPa and from 5.4 eV (cotunnite-type) to 5.0 eV (Fe_2P -type) at 600 GPa.

To inspect their dynamic stabilities, we also performed *ab initio* lattice-dynamics calculations for the pyrite, cotunnite, and Fe_2P structures at transition pressures based on the DFPT.²⁶ Calculated phonon-dispersion relations shown in Fig. 5 clearly indicate that the structures are dynamically stable with no imaginary frequencies. The maximum phonon frequency of Fe_2P -type (49.02 THz) is found to be slightly higher than that of cotunnite-type (45.78 THz). The GGA gives the same phonon properties with the maximum frequency of Fe_2P -type (48.51 THz) higher than that of cotunnite-type (45.42 THz). These phonon modes correspond to the Ge-O stretching motion, suggesting that the Ge-O bond is a little stronger in Fe_2P -type than in cotunnite-type. This is consistent with the contrasts of ECoN and the effective charges between these phases.

IV. CONCLUSIONS

We have investigated the structural phase transitions in GeO_2 based on the *ab initio* density-functional approach. Calculations have shown that a pyrite-to-cotunnite transition

occurs at 280 (281) GPa and a subsequent cotunnite-to- Fe_2P transition occurs at 589 (611) GPa within the LDA (GGA). While a substantial volume reduction contributes to the energetic stability of cotunnite and to driving the first transition, the volume is almost unchanged across the second transition. The cotunnite and Fe_2P -type structures are quite similar as both consist of GeO_9 polyhedra, which produce stable phonon frequencies at ultrahigh pressures. We have shown that the effective coordination number of Ge is closer to the apparent value of 9 in Fe_2P than in cotunnite, and the E_g and ionicity decrease across this phase transition. Unlike SiO_2 , the cotunnite-type structure is found to be adaptable to GeO_2 at moderate pressures even at static temperature. However, similarly to SiO_2 , the Fe_2P -type structure is more preferable at ultrahigh pressures primarily due to the structural regularity, suggesting that the Fe_2P -type structure is widely adaptable to dioxides under extreme pressure conditions.

ACKNOWLEDGMENTS

We thank S. Whitaker and anonymous reviewers for helpful comments. This work was supported by special coordination funds for promoting science and technology (Supporting Young Researchers with fixed-term Appointments) and in part by Japan Society for the Promotion of Science Grant-in-Aid for Scientific Research Grants 20001005 and 21740379.

¹J. Haines and J. M. Léger, *Phys. Rev. B* **55**, 11144 (1997).

²T. Tsuchiya, T. Yamanaka, and M. Matsui, *Phys. Chem. Miner.* **25**, 94 (1998).

³Z. Lodziana, K. Parlinski, and J. Hafner, *Phys. Rev. B* **63**, 134106 (2001).

⁴S. Ono, T. Tsuchiya, K. Hirose, and Y. Ohishi, *Phys. Rev. B* **68**, 014103 (2003).

⁵S. Ono, T. Tsuchiya, K. Hirose, and Y. Ohishi, *Phys. Rev. B* **68**, 134108 (2003).

⁶T. Tsuchiya, R. Caracas, and J. Tsuchiya, *Geophys. Res. Lett.* **31**, L11610 (2004).

⁷A. R. Oganov, M. J. Gillan, and G. D. Price, *Phys. Rev. B* **71**, 064104 (2005).

⁸Y. Kuwayama, K. Hirose, N. Sata, and Y. Ohishi, *Science* **309**, 923 (2005).

⁹S. J. Duclos, Y. K. Vohra, A. L. Ruoff, A. Jayaraman, and G. P. Espinosa, *Phys. Rev. B* **38**, 7755 (1988).

¹⁰J. Haines, J. M. Leger, S. Hull, J. P. Petit, A. S. Pereira, C. A. Perottoni, and J. A. H. da Jornada, *J. Am. Ceram. Soc.* **80**, 1910 (1997).

¹¹N. A. Dubrovinskaia, L. S. Dubrovinsky, R. Ahuja, V. B. Prokopenko, V. Dmitriev, H.-P. Weber, J. M. Osorio-Guillen, and B. Johansson, *Phys. Rev. Lett.* **87**, 275501 (2001).

¹²T. Sato, N. Funamori, T. Yagi, and N. Miyajima, *Phys. Rev. B* **72**, 092101 (2005).

¹³S. R. Shieh, A. Kubo, T. S. Duffy, V. B. Prakapenka, and G. Shen, *Phys. Rev. B* **73**, 014105 (2006).

¹⁴K. Umemoto, R. M. Wentzcovitch, and P. B. Allen, *Science* **311**, 983 (2006).

¹⁵T. Tsuchiya and J. Tsuchiya, *Proc. Natl. Acad. Sci. USA* **108**, 1252 (2011).

¹⁶P. Hohenberg and W. Kohn, *Phys. Rev.* **136**, B864 (1964).

¹⁷W. Kohn and L. J. Sham, *Phys. Rev.* **140**, A1133 (1965).

¹⁸D. M. Ceperley and B. J. Alder, *Phys. Rev. Lett.* **45**, 566 (1980).

¹⁹J. P. Perdew and A. Zunger, *Phys. Rev. B* **23**, 5048 (1981).

²⁰J. P. Perdew, K. Burke, and M. Ernzerhof, *Phys. Rev. Lett.* **77**, 3865 (1996).

²¹D. Vanderbilt, *Phys. Rev. B* **41**, 7892 (1990).

²²Electronic configurations for the pseudopotentials are $3d^{10}4s^24p^2$ for Ge and $2s^22p^4$ for O. Core cutoff radii are 1.3 and 1.6 a.u. for all l of O and Ge, respectively.

²³T. Tsuchiya, J. Tsuchiya, K. Umemoto, and R. M. Wentzcovitch, *Earth Planet. Sci. Lett.* **224**, 241 (2004).

²⁴T. Tsuchiya and J. Tsuchiya, *Phys. Rev. B* **76**, 092105 (2007).

²⁵P. Giannozzi *et al.*, *J. Phys. Condens. Matter* **21**, 395502 (2009).

²⁶H. J. Monkhorst and J. D. Pack, *Phys. Rev. B* **13**, 5188 (1976).

²⁷S. Baroni, S. de Gironcoli, A. D. Corso, and P. Giannozzi, *Rev. Mod. Phys.* **73**, 515 (2001).

²⁸K. Shiraki, T. Tsuchiya, and S. Ono, *Acta. Crystallogr.* **59**, 701 (2003).

²⁹C. Filippi, D. J. Singh, and C. J. Umrigar, *Phys. Rev. B* **50**, 14947 (1994).

³⁰R. Hoppe, *Z. Kristallogr.* **150**, 23 (1979).

³¹R. Bader, *Atoms in Molecules: A Quantum Theory* (Oxford University Press, New York, 1990).

³²M. Städele, M. Moukara, J. A. Majewski, P. Vogl, and A. Grling, *Phys. Rev. B* **59**, 10031 (1999)